Expanding holes driven by convectionlike flow in vibrated dense suspensions

H. Ebata,* S. Tatsumi,† and M. Sano‡
Department of Physics, Graduate School of Science, The University of Tokyo, Tokyo 113-0033, Japan
(Received 28 February 2009; revised manuscript received 5 May 2009; published 16 June 2009)

Surface instabilities in vertically vibrated suspensions of various powders dispersed in silicone oil are investigated in quasi-two-dimensional (2D) and quasi-one-dimensional (1D) systems. As vibration acceleration exceeded a critical value, the flat surface became unstable against a finite-amplitude perturbation. We found an expanding hole or viscous fingerlike pattern in the quasi-2D system and segregation between dried and wet areas in the quasi-1D system. We show that these instabilities are accompanied by convectionlike flow at their rim and in the quasi-1D system, the height of the convectionlike flow can be scaled by acceleration, vibration frequency, diameter of the dispersed powder, mean density of the suspension, and viscosity of silicone oil. We propose a simple model that accounts for the scaling and concentric motion of the convectionlike flow.

DOI: 10.1103/PhysRevE.79.066308 PACS number(s): 47.20.−k, 45.70.Mg, 45.70.Qj, 47.54.−r

I. INTRODUCTION

A hollow created on the flat surface of a fluid at rest eventually closes because of hydrodynamic pressure, even for non-Newtonian fluids such as suspensions. A free fluid surface that is parallel to the direction of gravity is hard to maintain using static-force balance and is absolutely unstable in general. Recently Merkt *et al.* discovered an interesting surface instability in vertically vibrated cornstarch or glass microsphere suspension [1]. They observed that a permanent hole is created by localized perturbation and persists despite the hydrodynamic pressure of the surrounding fluid. Here we report that such holes generally expand rather than just persist when the suspended glass beads are larger than a certain size. We found that convectionlike flow at the rim of the hole is responsible for maintaining the hole and thrusts the surrounding fluid out toward the wall against hydrodynamic pressure.

For a Newtonian fluid or granular medium, various surface instabilities are reported, such as Faraday waves [2], Rayleigh-Taylor instabilities [3], and oscillons [4]. Vertically vibrated suspensions also show those instabilities accompanied by features specific to particle-dispersion fluid systems. Oscillons and solitary waves are observed in clay suspensions [5], suggesting that the shear-thinning character of a suspension enhances the hysteresis of onset acceleration. Surface instabilities in the form of heaps accompanied by convection are documented for vertically vibrated granular slurries [6] and show that the critical acceleration of heaps results from a Rayleigh-Taylor instability.

In a vertically vibrated dense suspension of glass beads, we found that a finite localized perturbation destabilizes the surface above a certain threshold of acceleration, and a void created by the perturbation grows from the surface to nearly the bottom of the fluid layer, then expands from its initial diameter (∼5 mm) to almost the size of the container (∼30 cm) until it collides with the side wall of the container. The expanding hole resembles the dewetting of hydrophobic fluids [7] except that the wall of the expanding hole is sustained by a dynamic fluid process—that is, a convectionlike flow at the rim—and the height of the hole can reach much higher than for normal dewetting.

II. EXPERIMENT

For suspensions, we used mainly mixtures of glass beads and silicone oil. We varied the diameter of the beads r from 50 to 800 μm, the viscosity of the silicone oil η from 30 to 500 mm^2/s, and the packing fraction (also called the packing ratio) ϕ of the system from 45% to 61%. In some experiments, we used copper powder (mean diameter 200 μm) or polyethylene powder (mean diameter 100 μm) as dispersed particles. We used two types of acrylic-resin containers: a cylindrical container (diameter of 29 cm) for quasi-two-dimensional (2D) systems and a narrow box (10 $\times$ 1 cm^2) for quasi-one-dimensional (1D) systems. A layer of suspension (initial depth of 0.5–2.5 cm) was subjected to vertical sinusoidal vibration [vertical position $z(t) = A \sin 2\pi ft$] using an electromagnetic vibration system, where the frequency f was varied from 30 to 70 Hz and the peak acceleration $\Gamma \equiv A(2\pi f)^2$ was varied up to 280 m/s. This system shows a subcritical bifurcation, giving rise to a surface instability consisting of a hole.

We created a local perturbation by making a small hole in the flat surface with a stick and recorded the growth of instability in the system with a charge-coupled-device camera at 30 frames/s. A nonmatched density of glass beads and silicone oil can cause local nonuniformity in the packing fraction. To avoid this effect, the suspension poured in the container was mixed again within 30 s in prior to each experiment because typical sedimentation time is estimated to be 70 s for dilute suspensions by using Stoke's law, while the drag force is larger, thus it takes longer for dense suspensions. This experimental preparation time was enough to obtain reproducible result [8]. In the quasi-2D system, we mainly investigated the phase diagram and first-stage instabilities. In the quasi-1D system, we focused on the time evolution of instabilities and the steady state.

*ebata@daisy.phys.s.u-tokyo.ac.jp
†Also at Neutron Science Laboratory Institute for Solid State Physics, The University of Tokyo.
‡sano@phys.s.u-tokyo.ac.jp

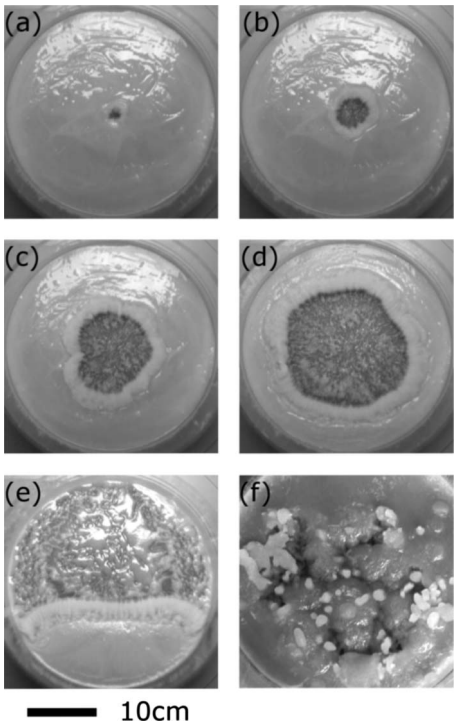

FIG. 1. Sequence of instabilities in a quasi-2D system: [(a)–(d)] Hole-expanding sequence at different times $t=0$, 2, 4, and 6 s (where $r=0.2$ mm, $\eta=500$ mm^2/s, $\phi=0.56$, $\Gamma=230$ m/s^2, and $f=40$ Hz); (e) separated state (where $r=0.2$ mm, $\eta=500$ mm^2/s, $\phi=0.56$, $\Gamma=290$ m/s^2, and $f=40$ Hz); (f) viscous fingerlike pattern (where $r=0.4$ mm, $\eta=500$ mm^2/s, $\phi=0.60$, $\Gamma=270$ m/s^2, and $f=60$ Hz).

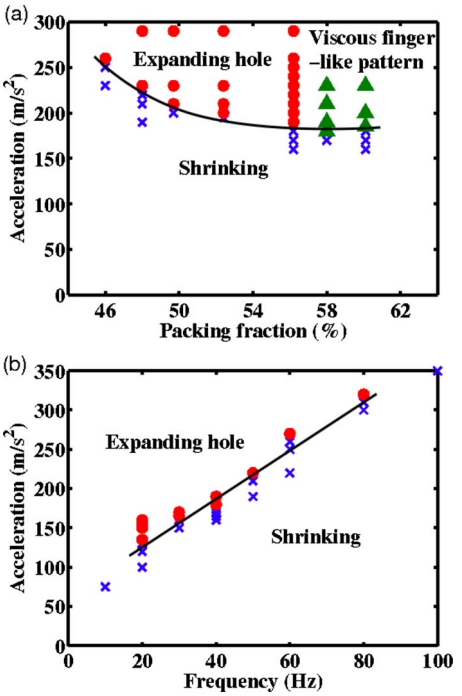

FIG. 2. (Color online) (a) Phase diagram of glass beads (0.2 mm) in silicone oil suspension (500 mm^2/s), shown as acceleration vs packing fraction. The vibration frequency was 40 Hz. An expanding hole is observed in the circle (red) symbol region and a viscous fingerlike pattern is observed in the triangle (green) symbol region. At packing fraction $\phi=58\%$, sometimes both expanding hole and viscous fingerlike pattern are observed simultaneously because of the nonuniformity of the packing fraction. (b) Phase diagram of glass beads (0.4 mm) in silicone oil suspension (500 mm^2/s), shown as acceleration vs frequency. The packing fraction $\phi=56\%$. In both figures, the expanding hole region (circles) indicates that the hole reaches the wall and the shrinking region (crosses) indicates that the hole starts shrinking. Near the onset of acceleration in the shrinking region, the hole can expand but starts shrinking.

When acceleration is sufficiently high, instability changes significantly with packing fraction. At lower packing fractions, a small hole [Fig. 1(a)] created by a finite perturbation grows into a large hole [Figs. 1(b)–1(d)] and finally, upon collision with the outer wall, into irregular forms. At higher packing fractions, the initial hole is followed by a front instability, creating many branches [Fig. 1(f)] that resemble viscous finger patterns in the Hele-Shaw cells [9] or peeling of adhesive tape [10]. We call the former an expanding hole and the latter a viscous fingerlike pattern. For a suspension of 0.2 mm glass beads, the threshold packing fraction ϕ_c is 58% [Fig. 2(a)]. The instabilities resemble hole growth in thin liquid films [7,11], and for $\phi>58\%$, sometimes both expanding hole and viscous fingerlike patterns coexist. The coexistence of two instabilities may be due to the nonuniformity of the packing fraction and is certainly due, in part, to the difficulty in establishing uniform initial conditions at very high packing fractions. However, particularly noticeable is the nonuniformity induced by instability. When the viscous fingerlike pattern appears, silicone oil is pushed out from the pattern region to the outer region and the uniformity of the packing fraction breaks spontaneously. At the advancing front, a granulated lump often tears off from the edge of the viscous fingerlike pattern [Fig. 1(f)]. When the concentrated suspension shears, the same granulation as that caused by dilatancy is observed [12]. Thus, it suggests that spontaneous breaking of uniformity of a packing fraction is due to dilation and granulation, which cause instability. The transition from a uniformly expanding hole to a hole with fingerlike patterns was observed for a packing fraction close to the onset of the hard-sphere glass transition that is found in a fluidized bed of hard spheres [13] and references therein. In the phase diagram, onset acceleration decreases monotonically with increasing packing fraction [Fig. 2(a)] [14]. Meanwhile, the onset acceleration of an expanding hole increases linearly with increasing frequency [Fig. 2(b)]. Hence, the onset acceleration is strongly affected by packing fraction and frequency but is not much affected by the diameter of the glass beads or the viscosity of the liquid. Even when we double the diameter of the glass beads, onset acceleration changes by only $\sim 5\%$. A mixture of copper beads and silicone oil with $\phi=56\%$ also demonstrates an expanding hole. However, if acceleration is insufficient, the hole expands slightly but then shrinks and soon disappears. In this study, we mainly focus on expanding holes. At the rim of all holes, convectionlike flow resembling a doughnut was found. We determined that the typical velocity of the flow is ~ 1 cm/s and that it increases with increasing Γ.

The flow goes upward along the hole rim and turns downward at some distance from the hole. We observed convection coupled with changing surface shape under vertical vibration, with rotational direction the reverse of [6] and the same as [15].

To make an expanding hole, a finite deformation of surface is indispensable. As the initial condition, usually it is necessary to make a hole penetrating the layer and there is a critical initial hole size below which a hole always shrinks. This critical initial hole size decreases with increasing acceleration; for example, with 0.1 mm glass beads in 100 mm^2/s silicone oil, the critical hole size is ~2.7 mm for acceleration 175 m/s^2 and 1.3 mm for acceleration 182 m/s^2. In contrast to the instabilities in [6,15] that show supercritical bifurcation, the necessity of a finite surface deformation indicates that this instability is subcritical.

For all experimental conditions, the growth of the area of the hole (S) is nonlinear with time [Fig. 3(a)]. However, the time-evolution curves collapse into a single growth curve at an early stage [Fig. 3(b)] when they are scaled.

We employ the functional form for the collapsed curve $S/S_0=f(t/\tau)$, where $f(x)=\exp(\sqrt{x})$, t is the elapsed time from the beginning of expansion, and τ is a parameter that is characteristic of the time scale of hole growth [Fig. 3(b)].

We fitted the data in Fig. 3(a) with fitting parameters τ and S_0. Figure 3(c) shows the relationship between τ and the external acceleration of the system, which reveals that τ diverges near the onset of acceleration. In the later stage of hole growth, the reaction from the wall becomes evident, and consequently, the scaling relationship is lost. At sufficiently high acceleration (>220 m/s^2 at 56%), the hole grows to roughly the size of the container and the rim of the hole collides with the container wall. In most cases, the hole shape is completely destroyed, and the suspension area and nonsuspension area (that is, the "dried area") separate [Fig. 1(e)]. We named this final state the "separated state." In the expanding hole and the separated state, convectionlike flow is always observed at the rim of the wall. The separated state seems strongly coupled with the strength of the convectionlike flow. Therefore, we focus on the dynamics of convectionlike flow and its relationship to the expanding hole in a quasi-1D system.

To study the detailed dynamics of detachment near the hole, we performed a quasi-1D experiment (Fig. 4). In a quasi-1D system, the separated state is observed above a certain acceleration. After the surface of the suspension is perturbed, the wall between the dried area and the suspension area moves toward the suspension area. The dried area begins to expand and the suspension area begins to compress until it is localized at one side of the wall (Fig. 4). We should note that since the thickness of a 1D cell is close to the minimum hole size of a 2D cell, the separated state in a 1D cell corresponds to that in a 2D cell, and the advancing wall in a 1D cell is thought to be the expanding hole in a 2D cell.

During the evolution of a system, three noticeable features appear only at the edge of the suspension area. One feature is the periodic breaking off from the bottom plate of the container with periodic external vibration (at the same frequency as the external vibration, typically 60 s^{-1}), which corresponds to the fast dynamics of this phenomenon. The

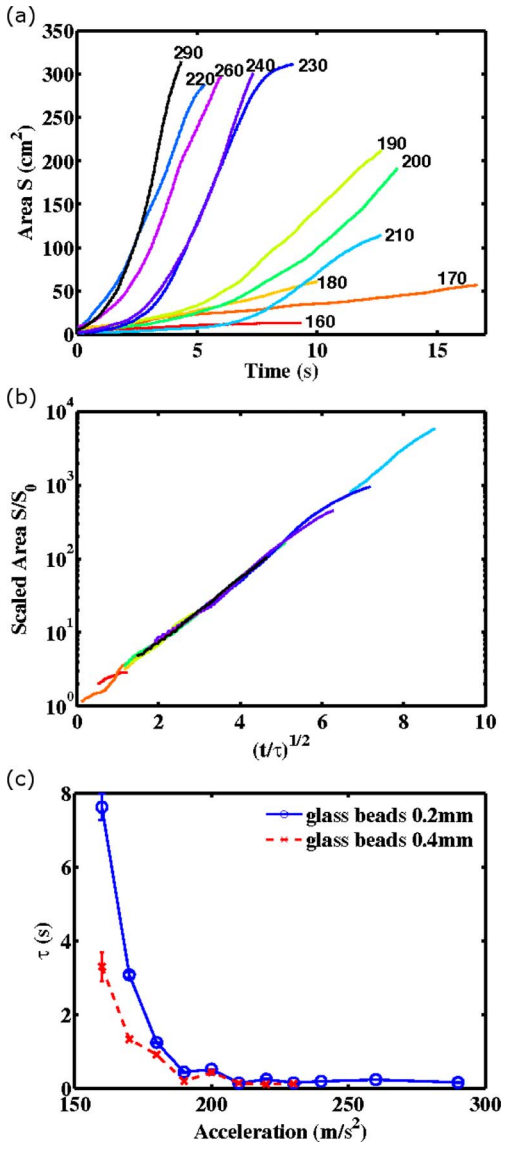

FIG. 3. (Color online) (a) Change in area with time for different accelerations. Γ varies from 160 to 240, 260, and 290 m/s^2. (b) Scaling of the first stage of time evolution. We cut the first one second to eliminate differences in the initial condition. In both (a) and (b), $r=0.2$ mm, $\eta=500$ mm^2/s, $\phi=0.56$, and $f=40$ Hz. The thickness of the layer is ~0.6 cm. (c) Change in the characteristic time scale τ with acceleration.

second feature is a rotational motion (on the order of 1 rotation/s), which corresponds to the slow dynamics of this phenomenon. In fact, in all of the investigated accelerations, periodic breaking off is completely synchronized with external vibration without any phase delay. However, the time scale of rotational motion, typically ~0.3 s^{-1}, is much slower than that of the fast dynamics. The third feature is the dependence of various parameters on the height of the edge, which corresponds to the height of the convectionlike flow. We found that the material constant, diameter of the glass beads, viscosity of silicone oil, energization parameter, frequency, and power of acceleration all affected the height of the edge. Only the total volume did not affect. Hereafter we focus on the height of the edge of steady flow.

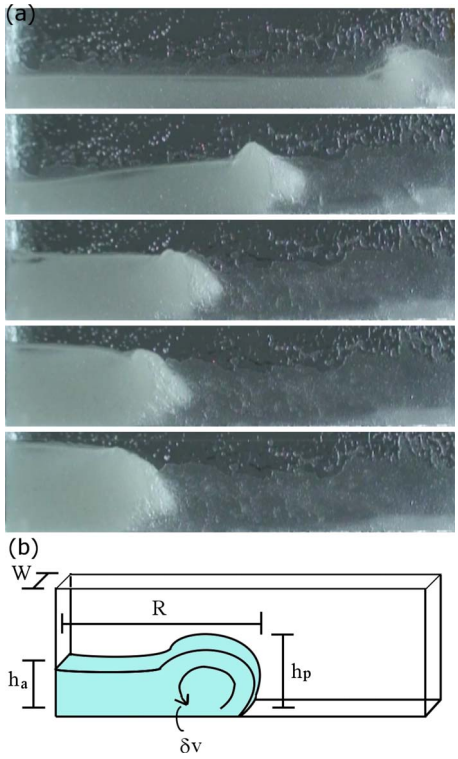

FIG. 4. (Color online) Time sequence in a quasi-1D system: (a) lateral view of the time sequence of separation at, from the top, $t=0$, 4, 8, 12, and 16 s; (b) frame format of the separated state and the convectionlike flow. R=convectionlike flow, h_a= mean height of the suspension region, h_p= height of the convection, and δv = velocity of circulation of the convectionlike flow.

III. THEORETICAL APPROACH

To explain the dependence of the parameters on the height of the edge, we derive a force-balance equation for the time evolution of separation with the following features:

(1) The rotation rate of the convectionlike flow is much slower than the vibration rate.

(2) The height of the convectionlike flow does not depend on the volume of the suspension.

(3) The height of the convectionlike flow increases with increasing viscosity.

(4) Only the rim oscillates by external vibration.

The first feature suggests that we consider only slow dynamics, so that all variables stand for time averages over a vibration cycle. The second and third features suggest that a balance between viscous stress on the wall and gravitational pressure determines the height of the convectionlike flow. Then, we introduce an equation of motion governing the location of the convectionlike flow R,

$$\frac{d}{dt}\rho V\dot{R} = -\eta^* h_p W\frac{\delta v}{d} - \eta^*(2\theta_D h_p^2 + h_p W)\frac{\dot{R}}{d} + \frac{1}{2}\rho g h_a^2 W, \tag{1}$$

where V is the volume of the rim, ρ is the density, η^* is the viscosity, δv is the typical velocity of circulation of the convectionlike flow, d is the width of boundary layer, h_p is the height of the rim, W is the width of the container, and h_a is the mean height of the suspension. Figure 4(b) shows a schematic picture for this model equation. On the right-hand side, the first term is a frictional force derived from convectionlike flow. The second term is a frictional force of concentric motion of the rim at the side walls and the bottom plate. The third term is the hydrostatic pressure due to gravity in the nonconvectional region. We assume that the time-averaged pressure quickly relaxes to the hydrostatic pressure in the nonconvectional region. Here, V can be written as $V=\theta_D h_p^2 W$, where θ_D is a fitting parameter, and we simply use $h_a = V_{tot}/(RW)$, where V_{tot} is the total volume of the suspension. Thus, we neglect the volume of the rim to calculate h_a. The velocity of the convectionlike flow is estimated by an energy balance. We assume that viscous dissipation occurs only at the boundary layer and, thus, obtain

$$\frac{\Delta E}{\Delta t} = \alpha\eta^* h_p^2\frac{\delta v^2}{d} + \eta^* h_p W\frac{\delta v^2}{d}, \tag{2}$$

where α is a fitting parameter. Equating this to the energy input per unit time by vertical vibration of the edge gives

$$\frac{\Delta E}{\Delta t} = \frac{1}{2}\rho V^*\frac{\Gamma^2}{\omega^2}\frac{\omega}{2\pi} = \frac{1}{4\pi}\rho V^*\frac{\Gamma^2}{\omega}, \tag{3}$$

where $V^*=\theta^* h_p^2$ is the volume that is vibrated by the external force.

Then, one arrives at

$$\delta v = \sqrt{\frac{\rho V^* d}{4\pi\eta^*(\alpha h_p^2 + h_p W)\omega}}\Gamma. \tag{4}$$

Finally, Eq. (1) becomes

$$\frac{d}{dt}\rho V\dot{R} = -h_p W\sqrt{\frac{\rho V^*\eta^*}{4\pi(\alpha h_p^2 + h_p W)\omega d}}\Gamma - \eta^* \times(2\theta_D h_p^2 + h_p W)\frac{\dot{R}}{d} + \frac{1}{2}\rho g h_a^2 W. \tag{5}$$

We now introduce three assumptions. First, viscosity η^* obeys the power law and is proportional to the viscosity of silicone oil η by the relationship $\eta^* \propto \eta(\omega/\omega_c)^{-n}$. Second, the thickness of the boundary layer is proportional to the diameter of the glass beads r. Third, the mean height h_a becomes equal to the height of the rim h_p and $\alpha h_p^2 \gg h_p W$. If we focus on the steady state, Eq. (5) leads to

$$h_p \propto \sqrt{\frac{\eta W\omega_c^n}{\rho r\omega^{1+n}}}\frac{\Gamma}{g}. \tag{6}$$

This model does not describe the mechanism of convectionlike flow. Consequently, the model can be applied only for the motion of the edge and does not explain the onset of convectionlike flow. Figure 5(a) shows the time evolution of the rim location R and the fitting curve calculated by Eq. (5), and uses three fitting parameters: α, θ_D, and $\theta_D^*\omega_c^n$. In contrast to the time evolution of the expanding hole in a quasi-2D system [Fig. 3(a)], the motion of the separation process in a quasi-1D system is very slow, probably because of frictional force from the walls. [Note that the curve in Fig.

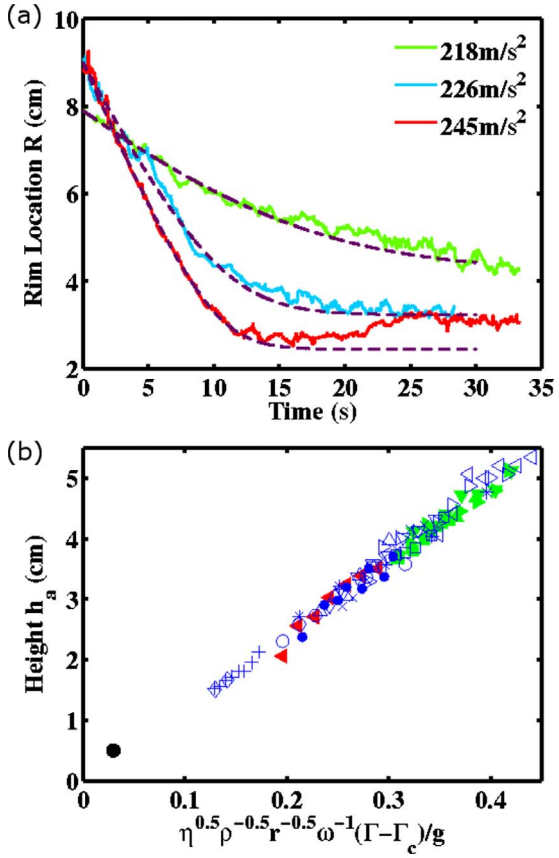

FIG. 5. (Color online) Time evolution of front propagation and scaling in a quasi-1D cell: (a) time evolution of the front propagation. The vertical axis is the length of the suspension area R. The diameter of the glass beads is 0.2 mm; the viscosity of the silicone oil is 100 mm^2/s; the dashed line is a fitting curve using Eq. (5). (b) Scaling of the height of the convectionlike flow. The large black bullet represents a stable hole in cornstarch and CsClaq suspension from [1]. For all data except cornstarch suspension, the packing fraction ϕ is 56%. The total volume of suspension in each data is different. However, at a sufficient total volume, the height of the suspension becomes almost independent of total volume: + (60 Hz, 100 mm^2/s, 0.2 mm, 1.83 g/cm^3); ○ (60 Hz, 100 mm^2/s, 0.1 mm, 1.83 g/cm^3); ∗ (60 Hz, 100 mm^2/s, 0.05 mm, 1.83 g/cm^3); • (blue/gray) (60 Hz, 236 mm^2/s, 0.2 mm, 1.83 g/cm^3); × (60 Hz, 358 mm^2/s, 0.2 mm, 1.83 g/cm^3); □ (60 Hz, 500 mm^2/s, 0.2 mm, 1.83 g/cm^3); ◇ (70 Hz, 100 mm^2/s, 0.2 mm, 1.83 g/cm^3); △ (50 Hz, 100 mm^2/s, 0.2 mm, 1.83 g/cm^3); ▽ (40 Hz, 100 mm^2/s, 0.2 mm, 1.83 g/cm^3); ▷ (30 Hz, 100 mm^2/s, 0.2 mm, 1.83 g/cm^3); ◁ (20 Hz, 100 mm^2/s, 0.2 mm, 1.83 g/cm^3); ■ (60 Hz, 30 mm^2/s, 0.1 mm, 0.957 g/cm^3); ▲ (50 Hz, 30 mm^2/s, 0.1 mm, 0.957 g/cm^3); ▼ (40 Hz, 30 mm^2/s, 0.1 mm, 0.957 g/cm^3); ▶ (30 Hz, 30 mm^2/s, 0.1 mm, 0.957 g/cm^3); ◀ (60 Hz, 500 mm^2/s, 0.2 mm, 5.46 g/cm^3).

3(a) shows the time evolution of the hole region, while the curve in Fig. 5(a) shows the time evolution of the suspension region.] As shown in Fig. 5(b), the experimental data were fitted as

$$h_p \propto \eta^{0.5}\rho^{-0.5}r^{-0.5}\omega^{-1}(\Gamma - \Gamma_c). \tag{7}$$

The scaling exponents are consistent with Eq. (6), suggesting that glass beads and silicone oil suspension show shear thinning with the exponent $n=1$. This frequency dependence agrees with the result in the oscillatory experiments [5,16]. However, those experiments deal with less concentrated suspensions ($\phi=0.4$ and $\phi=0.155-0.185$), so we need to check the exponent with a dense suspension at $\phi=0.56$. In addition, the scaling of the experimental data in Fig. 5(b) has onset acceleration Γ_c. A conceivable cause for this is excess energy dissipation by a convectionlike flow for $\Gamma >= \Gamma_c$. We examined this fitting for the stable hole in a cornstarch suspension in [1]. The large black bullet in Fig. 5(b) represents the data from [1]. $\Gamma_c=0$ is chosen for the cornstarch suspension, and the diameter of the hole is chosen for W. Although the data of [1] is obtained in a quasi-2D system and the packing fraction differs from ours, this fitting seems to be consistent with the height of the stable hole in a cornstarch suspension. We did a supplemental experiment with cornstarch and CsClaq suspension in a quasi-2D system and found convectionlike flow around the stable hole. We also examined a nondensity-matched cornstarch suspension and a hollow glass bead (13 μm in diameter) suspension, and found a stable hole that was, however, slightly less stable than the density-matched cornstarch suspension. Thus, the supplemental experiment and the fitting imply that a stable hole in a cornstarch suspension and an expanding hole or separated state in other suspensions have similar mechanisms. Finally, Eqs. (5) and (6) enable us to explain the motion of the edge and height of the edge in a steady state and indicate that viscous stress plays an important role in the separate state and the hole.

IV. DISCUSSION AND CONCLUSION

To conclude, we found the following types of surface instability in vertically vibrated dense suspensions: an expanding hole, a viscous fingerlike pattern, and a separated state. At the rim of the expanding hole and the separated state, there exists convectionlike flow. We observed a transition from the expanding hole to a viscous fingerlike pattern with increasing packing fraction. We propose that these instabilities enhance the nonuniformity of the packing fraction and that the occurrence of nonuniformities in suspensions causes the coexistence of different states. This conjecture should be tested by a controlled experiment to elucidate the connection among this transition, dilation, and particle flux [17]. In a quasi-1D system, we found scaling for the height of the edge, suggesting that convectionlike flow and its viscous stress expands or sustains the hole. Rheological measurement is still needed to confirm the model and to clarify whether glass beads in silicone oil suspension show shear thinning with varying frequency. A critical remaining problem is how convectionlike flow at the rim emerges. Shiba *et al.* [15] found convection in vertically vibrated viscoplastic fluids and showed that the magnitude of the critical inertial stress coincides with the yield stress of viscoplastic fluids. Meanwhile, experiments with cornstarch suspension [1] indicate that a stable hole appears at a shear-thickening region. The mechanism of the onset of convectionlike flow or a

stable hole in [1] is not elucidated, and the relationship between the dynamics of suspension and rheology is not yet resolved. Exploration of the dynamics of dense suspensions began recently, with many groups investigating the rheology of suspensions both theoretically and experimentally [18–23]. There still remains a need for further research into the dynamics of dense suspensions and into the connection between dynamics and rheological properties of dense suspensions. Further experiments are now in progress to elucidate the mechanism of convectionlike flow.

ACKNOWLEDGMENTS

The authors would like to thank Shin-iti Nakasuka for letting us use his laboratory facilities to perform 2D experiments. This work is supported by a Grant-in-Aid for Scientific Research (Grant No. 18068005) from MEXT Japan.

[1] F. S. Merkt, R. D. Deegan, D. I. Goldman, E. C. Rericha, and H. L. Swinney, Phys. Rev. Lett. **92**, 184501 (2004).
[2] M. Faraday, Philos. Trans. R. Soc. London **121**, 299 (1831).
[3] G. I. Taylor, Proc. R. Soc. London, Ser. A **201**, 192 (1950).
[4] P. Umbanhowar, F. Melo, and H. L. Swinney, Nature (London) **382**, 793 (1996).
[5] O. Lioubashevski, Y. Hamiel, A. Agnon, Z. Reches, and J. Fineberg, Phys. Rev. Lett. **83**, 3190 (1999).
[6] J. M. Schleier-Smith and H. A. Stone, Phys. Rev. Lett. **86**, 3016 (2001).
[7] G. Debrégeas, P. Martin, and F. Brochard-Wyart, Phys. Rev. Lett. **75**, 3886 (1995).
[8] The nonmatched density of glass beads and silicone oil could affect the result. We therefore performed experiments in quasi-1D and quasi-2D systems with density-matched suspensions using 100 μm polyethylene powder (0.958 g/cm^3) and 30 mm^2/s silicone oil (0.955 g/cm^3). We found no significant difference in the result between the non-density-matched and density-matched suspensions, and we conclude that sedimentation is not crucial.
[9] J. Nittmann, G. Daccord, and H. E. Stanley, Nature (London) **314**, 141 (1985).
[10] Y. Yamazaki and A. Toda, J. Phys. Soc. Jpn. **71**, 1618 (2002).
[11] B. M. Besancon and P. F. Green, Phys. Rev. E **70**, 051808 (2004).
[12] M. E. Cates, M. D. Haw, and C. B. Holmes, J. Phys.: Condens. Matter **17**, S2517 (2005).
[13] D. I. Goldman and H. L. Swinney, Phys. Rev. Lett. **96**, 145702 (2006).
[14] If we wait more than a few minutes after stirring, which is comparable to sedimentation time, the onset acceleration is constant at ~ 190 m/s^2 and shows no dependence on the mean packing fraction. In this case, the local packing fraction near the bottom becomes higher than the mean packing fraction, so the lack of dependence of the mean packing fraction implies that the local packing fraction near the bottom, rather than the mean packing fraction, determines the onset acceleration.
[15] H. Shiba, J. E. Ruppert-Felsot, Y. Takahashi, Y. Murayama, Q. Ouyang, and M. Sano, Phys. Rev. Lett. **98**, 044501 (2007).
[16] P. Rigord, E. Charlaix, and L. Petit, J. Phys. II **6**, 1091 (1996).
[17] Z. W. Fang, A. A. Mammoli, J. F. Brady, M. S. Ingber, L. A. Mondy, and A. L. Graham, Int. J. Multiphase Flow **28**, 137 (2002).
[18] A. Fall, N. Huang, F. Bertrand, G. Ovarlez, and D. Bonn, Phys. Rev. Lett. **100**, 018301 (2008).
[19] G. Ovarlez, F. Bertrand, and S. Rodts, J. Rheol. **50**, 259 (2006).
[20] D. Lootens, H. Van Damme, and P. Hébraud, Phys. Rev. Lett. **90**, 178301 (2003).
[21] J. Hyväluoma, P. Raiskinmäki, A. Koponen, M. Kataja, and J. Timonen, Phys. Rev. E **72**, 061402 (2005).
[22] D. Lootens, H. van Damme, Y. Hémar, and P. Hébraud, Phys. Rev. Lett. **95**, 268302 (2005).
[23] S. R. Raghavan and S. A. Khan, J. Colloid Interface Sci. **185**, 57 (1997).